Jurnal Teknologi

Full paper

Effect of Obstacle Position and Porous Medium for Heat Transfer in an Obstructed Ventilated Cavit

Mousa Farhadi*, Abbasali Abouei Mehrizi, Korush Sedighi, Hamid Hasanzadeh Afrouzi

[a]*Faculty of Mechanical Engineering, Babol University of Technology, Babol, Islamic Republic of Iran*

*Corresponding author: mfarhadi@nit.ac.ir

Article history

Received :15 June 2012
Received in revised form :12 August 2012
Accepted :28 August 2012

Graphical abstract

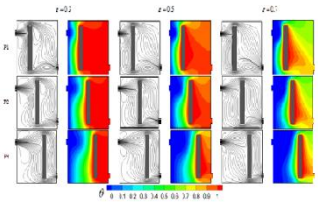

Abstract

In this paper, heat transfer enhancement in an obstructed ventilated cavity using porous medium was investigated. The lattice Boltzmann method was used to simulate forced convection in clear and porous domain. The Brinkman Forchheimer model was performed to simulate porous medium. The walls of cavity in addition to inlet and outlet port are thermally insulated and the obstacle is maintained at constant temperature. The simulation was carried out for different Reynolds and Prandtl numbers in the range of 20 to 60 and 0.7 to 5, respectively. Furthermore the effects of different positions of obstacle and different porosity values on thermal field, flow field and Nusselt number were studied. The Results show that by adding the porous medium to the domain and decreasing porosity, heat transfer enhances. Also by augmentation of Reynolds and Prandtl numbers the value of average Nusselt number increases. Furthermore the result points that the obstacle position has important effect on heat transfer rate. The best position of obstacle to reach the maximum heat transfer rate is Position 1.

Keywords: Convective heat transfer, Lattice Boltzmann Method (LBM), porous media, vented cavity, Brinkman Forchheimer model

1.0 INTRODUCTION

Forced convection heat transfer in porous media has attracted many scientist and researcher during the past several decades because of its wide range of applications. The porous medium are usually used for improving heat transfer in industry such as nuclear Reactors cooling, heat pipes, packed bed reactors, heat exchangers, geothermal and electronic cooling.

Bejan [1] reviewed many investigations about the forced convection and a complete review about convective heat transfer in porous media were published by Nield and Bejan [2] and Vafai [3]. Several forced convection heat transfer problems were studied in different geometries which were partially filled or fully filed with porous medium. Hwang *et al*. [4] performed numerical and experimental study of heat transfer in channel filled with sintered metals. An experimental study of heat transfer characteristic in porous channel filled with sintered metal was developed by Jiang *et al*. [5]. Furthermore the problem was solved numerically by Jiang and Lu [6]. The results indicate that porous media has a strong effect on enhancing heat transfer. By adding the porous media in the domain, the local heat transfer coefficient grows up to 15 times for water and 30 times for air.

The heat transfer in ventilated cavity has not been investigated widely. The heat transfer due to the flow over two porous blocks situated in a ventilated square cavity was investigated by Shuja *et al*. [7]. They found that increasing porosity of the blocks modifies the flow field in the cavity and the Nusselt number enhances with the increasing porosity and heat flux. The Results also indicated that a smaller particle diameter can be used to achieve higher heat transfer enhancement.

Hadim and North [8] presented a laminar forced convection in a sintered porous channel with inlet and outlet slots. They investigated the effects of particle diameter, Reynolds number, and channel dimensions.

Forced convection in a square cavity with inlet and outlet ports was investigated by Saeidi and Khodadadi [9-10]. They developed a finite-volume-based computational study of transient laminar flow and heat transfer leading to periodic state within a square cavity with inlet and outlet ports due to an oscillating velocity at the inlet port. They also investigated the effect of outlet port position on thermal and flow filed as a separated study. The Lattice Boltzmann method is a numerical recently developed method which is obtained adequate result in simulation of complex phenomena in fluid mechanics [11-20]. Guo and Zhao [17] applied the lattice Boltzmann method to simulate heat transfer and fluid flow in porous media. They successfully simulated the Poiseuille flow, Couette flow and Lid-driven cavity flow. Seta *et al*. [18, 19] used the Brinkman Forchheimer model to solve natural convection in square cavity filled with porous medium and showed heat behavior variation with porosity, Darcy

and Rayleigh numbers. Javaran *et al*. [20] successfully modeled the two-dimensional heat recovery system using porous media by Lattice Boltzmann method. Porous medium was modeled by gas and solid phases and two different thermal distribution functions.
The aim of this paper is the investigation of forced convection heat transfer in a vented square cavity, with a hot obstacle and filled with porous medium using Lattice Boltzmann method. The effects of fin position and porosity values are examined on heat transfer characteristics at different Reynolds and Prandtl numbers.

2.0 Lattice Boltzmann Method for Incompressible Flow in Porous Media

The LBM is classified in computational fluid dynamics (CFD) methods. In contrast to the classical macroscopic Navier Stokes (NS) approach, the Lattice Boltzmann Method (LBM) uses a mesoscopic simulation model to simulate fluid flows.
The general form of Lattice Boltzmann equation with external force can be written as:

$$f_k(\vec{x}+\vec{c}_k\Delta t, t+\Delta t) - f_k(\vec{x},t) = \Delta t \frac{f_k^{eq}(\vec{x},t) - f_k(\vec{x},t)}{\tau} + \Delta t.\vec{F}_k \quad (1)$$

Where Δt denotes lattice time step, $\vec{c}_k$ is the discrete lattice velocity in direction *k*, F_k is the external force in direction of lattice velocity $\vec{c}_k$, τ denotes the lattice relaxation time, f_k^{eq} is the equilibrium distribution function. The local equilibrium distribution function determines the type of problem that needs to be solved.
Eq. (1) is usually solved in two steps:

$$f_k(\vec{x},t+\Delta t) - f_k(\vec{x},t) = \Delta t \frac{f_k^{eq}(\vec{x},t) - f_k(\vec{x},t)}{\tau} + \Delta t.\vec{F}_k \quad (2)$$

$$f_k(\vec{x}+\vec{c}_k\Delta t, t+\Delta t) = f_k(\vec{x},t+\Delta t) \quad (3)$$

Eqs. (2) and (3) are called the collision and streaming steps, respectively. The collision step models various fluid particle interactions like collisions and calculates new distribution functions according to the distribution functions of the last time step.
For simulation the fluid flow in the porous medium many models are developed. Neild and Bejan derived the Brinkmane-Forchheimer equation which includes the viscous and inertial terms by the local volume averaging technique [2]. This model has been used successfully in simulation porous media in wide range of porosities, Rayleigh, Reynolds and Darcy numbers [18, 19, 21].The Brinkmane-Forchheimer equation is written as:

$$\frac{\partial \vec{u}}{\partial t} + (\vec{u}\cdot\nabla)\left(\frac{\vec{u}}{\varepsilon}\right) = -\frac{1}{\rho}\nabla(\varepsilon p) + \upsilon_{eff}\nabla^2\vec{u} + \vec{F} \quad (4)$$

Where ε is the porosity of the medium, and υ_{eff} the effective viscosity, $\vec{F}$ is the total body force and contains the viscous diffusion, the inertia due to the presence of a porous medium, and an external force which with the widely used Ergun's relation can be written as [18,19,22]:

$$\vec{F} = -\frac{\varepsilon\upsilon}{K}\vec{u} - \frac{1.75}{\sqrt{150\varepsilon K}}|\vec{u}|\vec{u} \quad (5)$$

Where υ is the kinematic viscosity and *K* is the permeability. The permeability is related to Darcy number (*Da*), and the characteristic length (*H*) with:

$$k = DaH^2 \quad (6)$$

The equilibrium distribution functions are calculated by:

$$f_k^{(eq)} = \omega_k\rho\left[1 + \frac{\vec{c}_k.\vec{u}}{c_s^2} + \frac{1}{2}\frac{(\vec{c}_k.\vec{u})^2}{\varepsilon c_s^4} - \frac{1}{2}\frac{\vec{u}^2}{\varepsilon c_s^2}\right] \quad (7)$$

It was shown that the best choice for the forcing term F_k to achieve correct equation of hydrodynamics is taken [17, 18, 23]:

$$F_k = \omega_k\rho\left(1 - \frac{1}{2\tau_\upsilon}\right)\left[\frac{\vec{c}_k.\vec{F}}{c_s^2} + \frac{(\vec{u}\vec{F}:\vec{c}_k\vec{c}_k)}{\varepsilon c_s^4} - \frac{\vec{u}.\vec{F}}{\varepsilon c_s^2}\right] \quad (8)$$

The forcing term F_k defines the fluid velocity $\vec{u}$ as [18, 19]:

$$\vec{u} = \sum_k \frac{c_k F_k}{\rho} + \frac{\Delta t}{2}\vec{F} \quad (9)$$

According to the above equations, $\vec{F}$ is related to $\vec{u}$, so the Eq. (9) is nonlinear for the velocity. Guo and Zhao presented a temporal velocity $\vec{v}$ to solve this nonlinear problem as follows [17]:

$$\vec{u} = \frac{\vec{v}}{c_0 + \sqrt{c_0^2 + c_1|\vec{v}|}}, \qquad \vec{v} = \sum_k \frac{c_k f_k}{\rho} \quad (10)$$

$$c_0 = \frac{1}{2}\left(1 + \varepsilon\frac{\Delta t\,\upsilon}{2K}\right), \qquad c_1 = \varepsilon\frac{\Delta t}{2}\frac{1.75}{\sqrt{150\,\varepsilon^3 K}} \quad (11)$$

The Lattice Boltzmann equation for thermal energy distribution can be written as below:

$$g_k(\vec{x},t+\Delta t) - g_k(\vec{x},t) = \Delta t \frac{g_k^{eq}(\vec{x},t) - g_k(\vec{x},t)}{\tau_c} \quad (12)$$

For thermal simulation the three equilibrium distribution functions were used [18].

$$g_0^{eq} = -\frac{2\rho\vec{c}_k}{3}\frac{\vec{u}^2}{c^2} \quad (13)$$

$$g_i^{eq} = -\frac{\rho e}{9}\left[\frac{3}{2} + \frac{1}{2}\frac{\vec{c}_k.\vec{u}}{c_s^2} + \frac{1}{2}\frac{(\vec{c}_k\cdot\vec{u})^2 - c_s^2\vec{u}^2)}{c_s^4}\right] \qquad (i = 1,2,3,4)$$

$$g_i^{eq} = -\frac{\rho e}{36}\left[3 + 3\frac{\vec{c}_k.\vec{u}}{c_s^{\,2}} + \frac{1}{2}\frac{(\vec{c}_k\vec{u})^2 - c_s^2\vec{u}^2)}{c_s^4}\right] \qquad (i = 5,6,7,8) \tag{14}$$

3.0 NUMERICAL PROCEDURE

3.1 Boundary Conditions

In the simulation of model, the flow is assumed steady, two dimensional, incompressible and laminar. The computational domain is considered a vented square cavity and one obstacle. The obstruction was located at the center of the cavity. Domain is filled with the porous medium except the inlet and outlet port (Figure 1). Width of inlet and outlet ports is H like the obstacle, the distance of inlet port from the floor of the cavity is 8H, this distance for the outlet port is 2H. The length of inlet and outlet ports is 5H to get the fully developed flow in inlet and outlet ports. The walls of the cavity and ports are adiabatic and the obstacle is maintained at constant high temperature (T_h) and temperature of inlet flow was set at low temperature (T_c).

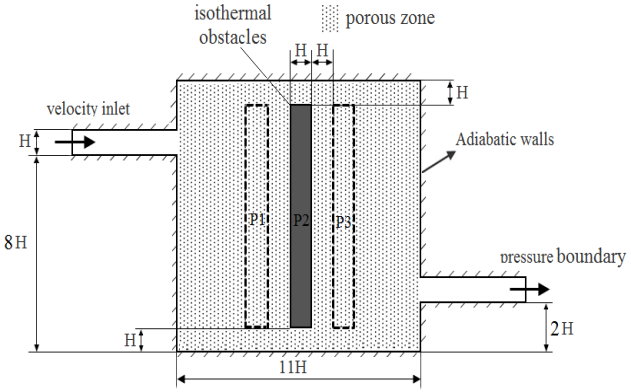

Figure 1 Schematic diagram of the physical system

3.1 Validation

In this study for validation of numerical simulation, the fluid flow in the full porous channel and natural convection in a square cavity filled with porous medium is simulated. The result of non dimensional velocity profile for different Reynolds and Darcy number were plotted at the Figure 2 (a) and (b). The compare of present study with previous study [18, 24] shows a good agreement. The average Nusselt number at different Rayleigh numbers were compared with seta [17] and Nithiarasu *et al*. works [25] in Figure 2 (c).

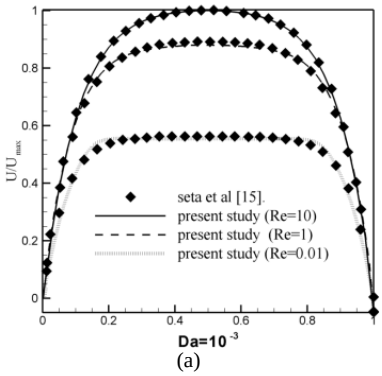

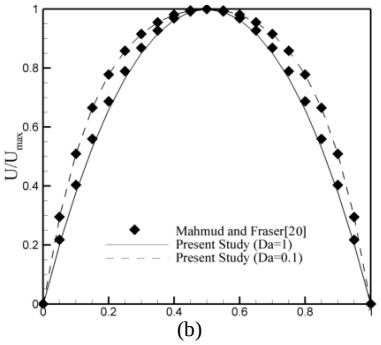

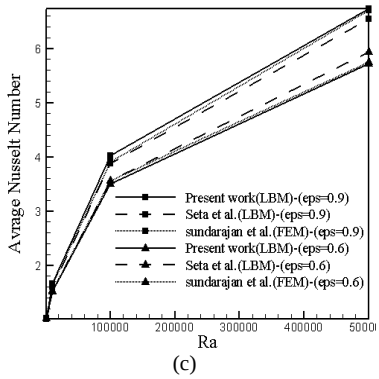

Figure 2 Dimensionless velocity profiles for: (a) Full porous channel at various Reynolds number,(b) Full porous channel at various Darcy number, (c) validation of Average Nusselt number for natural convection in cavity.

4.0 RESULTS AND DISCUSSION

As shown in Figure 3, the flow owing high momentum goes through inlet narrow port into the cavity. Then, the flow is affected by a sudden expansion which makes a positive pressure gradient. Therefore, two recirculation cells appear at the top and bottom sections of the inlet flow. It should be mentioned that the size of the lower vortex is larger than upper vortex. Then the flow moves to top and down of the obstacle and passes from the narrow section (distance between obstruction walls and cavity walls). Afterward, the flow is affected by another sudden expansion which makes the circulation region behind the obstacle.

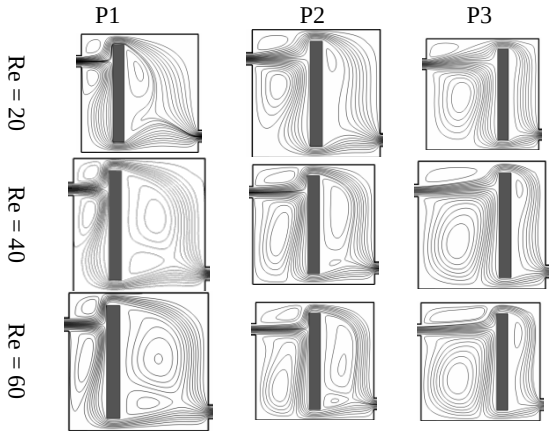

Figure 3 Streamlines at different Reynolds number and obstacle Positions when Pr=0.7 and $\varepsilon = 1$

Figure 3 shows the streamlines pattern at different obstruction positions and Reynolds numbers. With the increase of Reynolds number, the size of vortices grows up. The core of vortexes at the left side of obstacle grows, and consequently enforcing the flow to have better contact with left surface of obstacle and leading to increase heat transfer rate.

Obstacle position has significant effect on streamlines pattern. At P1, the distance between the left side of obstacle and cavity walls is restricted. So, the vortices near the inlet port are small. At Re=20 only a vortex appears behind the obstacle but at the higher Reynolds number, due to the augmentation of fluid momentum, another recirculation area appears near the right side of obstacle. This phenomenon can be observed by locating the obstacle at P2. By changing the obstacle position from P1 to P3, the distance between the left side of obstacle and cavity walls is grown and the opposite space is restricted. So, the vortices at the left of obstruction grow and the cores of vortices move to right.

By increasing the Reynolds number, the core of vortex placed behind the obstruction extends along the surface. Finally, at the high Reynolds number, the vortex covers completely the surface. This phenomenon increases the heat transfer rate.

The effect of obstacle position on thermal field at different Reynolds number is demonstrated in figure 4. This figure shows that the Reynolds number and fin position have essential effect on temperature contours. At low Reynolds number (Re=20) only one plume appears at the right side of obstacle but by increasing the Reynolds number two plumes arise from the top and downside at the right surface of the obstacle. By changing the obstacle position from P1 to P3 these two plumes reduce to one plume near the outlet port. Furthermore, more deflection is observed on the isotherms at the left side of obstacle.

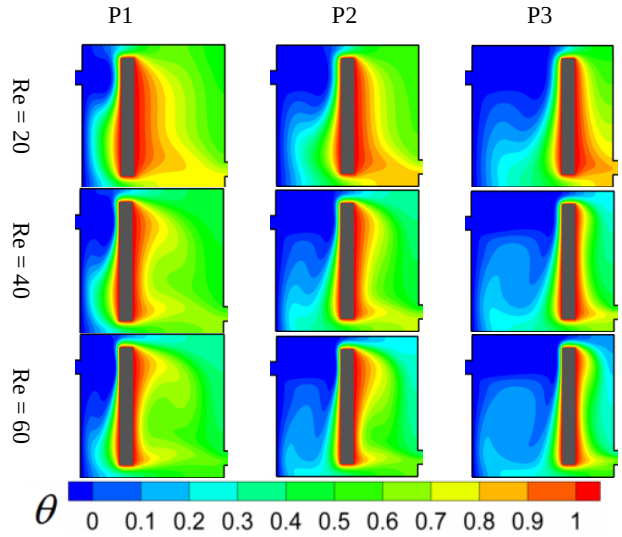

Figure 4 Temperature contours at different Reynolds number and obstacle Positions when Pr=0.7 and $\varepsilon = 1$

Figure 5 shows the effect of Prandtl number on heat transfer and temperature contours. With increase of the Prandtl number and decreasing the thermal diffusivity, the heat penetration decreases in the fluid flow. So, at the high Prandtl number, the fluid goes out without heat absorption. Adding the porous medium has sensible effect on heat transfer. The porous medium decreases the momentum of fluid, so flow has enough time to get the heat from the obstacles. This makes better heat transfer and increases the temperature of outlet flow (figure 6).

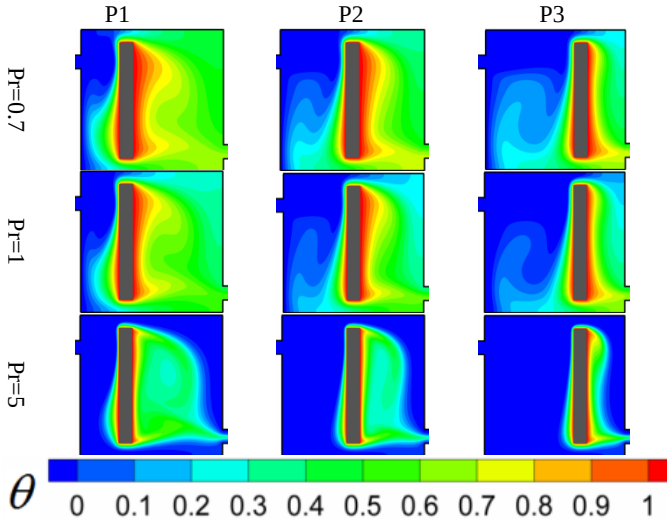

Figure 5: Temperature contours at different Prandtl number and obstacle Positions when Re=40 and $\varepsilon = 1$

Figure 6 shows the streamlines and temperature contours with different porosity and different obstacle positions. The streamlines indicate that as the porosity values decrease the size of vortices increases. The other important point is increment of effective thermal conductivity of fluid by reduction of porosity. As a result, the heat transfer rate increases. In addition, the temperature contours show that by reduction of the porosity the plume is removed.

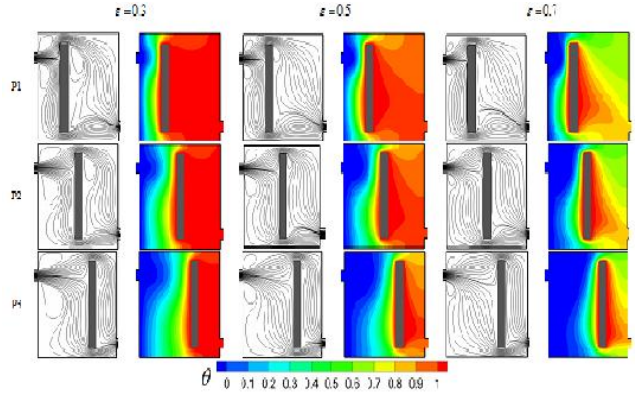

Figure 6 Streamline and temperature contours at different porosities value and different obstacle positions when Re=40 and Pr=1

Variation of average Nusselt number versus the porosity at the different Reynolds and Prandtl numbers and different obstacle position is presented in Figure 7. The local and average Nusselt number for obstacle is defined as:

$$Nu = \frac{hL}{k_f} = \left(\frac{k_{eff}}{k_f}\right)\left.\frac{\partial\theta}{\partial n}\right|_w \qquad (16)$$

$$Nu_{avg} = \frac{1}{l}\int_0^l Nu\ ds \qquad (17)$$

Where k_{eff} is effective conductivity, k_f is fluid conductivity, L=11H is characteristic length and θ is dimensionless temperature.

It is observed that the average Nusselt number increases with the reduction of porosity and increment of Prandtl and Reynolds numbers. The result indicates that the obstacle position has a little effect on Nusselt number at clear domain and high porosity values ($\varepsilon = 0.9$), but at lower porosity the obstacle position plays an important role in amount of heat transfer.

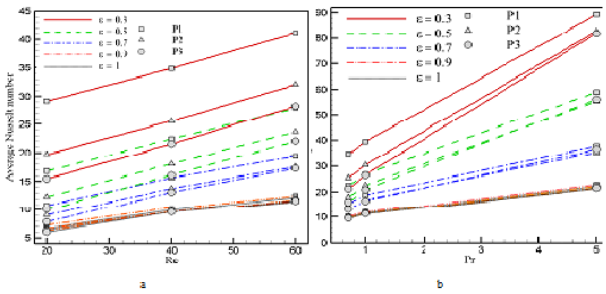

Figure 7 Variation of Average Nusselt number for different values of Porosity and different positions of obstruction, when: (a) Pr=0.7 versus the Reynolds number (b) Re=40 versus the Prandtl number.

Figure 7 shows that the position 1 is the best position on obstacle to reach the better heat transfer rate at all Reynolds and Prandtl numbers and porosity values. When the obstacle is located at P2, the Nusselt number is greater than of position 3 at high porosity values. But at $\varepsilon = 0.9$ and $\varepsilon = 1$ the Nusselt number is approximately equal for P2 and P3. Furthermore at low Prandtl number this phenomenon is observed but at high Prandtl number (Pr=5) and low porosities ($\varepsilon = 0.3$ and $\varepsilon = 0.5$) the Nusselt number at P2 and P3 is equal, approximately. But at higher porosity values the obstacle has better heat transfer rate at P3 in comparison with P2. Finally, it is shown that the maximum difference between the value of average Nusselt numbers occurs at Re=20 for $\varepsilon = 0.3$ and $\varepsilon = 1$ (Pr=0.7) when the obstacle is located at P1. For this difference the ratio of average Nusselt number grows 4.36 times. For the Prandtl number the maximum difference occurs for Pr=5 (Figure 6-b) which this ratio equals to 4.03.

5.0 CONCLUSIONS

The effect of porous medium and obstacle position on improvement of heat transfer characteristic was investigated by the Lattice Boltzmann method. The Brinkman-Forchheimer model was used for simulation of porous medium. The study was validated by comparing non-dimensional velocity in simulated full porous channel and average Nusselt number in a natural convection in square cavity with previous works. The effects of Reynolds and Prandtl numbers and porosity values in addition to obstacle position were studied. The results indicate that the porous medium has suitable effect on enhancement of heat transfer at different obstacle positions. The best position of obstacle to reach the highest Nusselt number is P1. Finally, it was found that by augmentation of the Reynolds and Prandtl numbers and reduction of the porosity, the Nusselt number increases.

Nomenclature

c	-discrete lattice velocity, [m^2 / s]	Greek symbols	
f	-distribution function for flow, [-]	ε	-the porosity of porous media[-]
F	-total body force, [-]	υ	-kinematic viscosity, [m^2 / s]
g	-distribution function for temperature, [-]	ρ	-Density, [kg / m^3]
K	-permeability , [m^2]	τ	-relaxation time, [-]
n	-the normal direction on the wall surface[-]	ω	-weighting factor, [-]
Nu	-Nusselt number, [-]	Subscripts	
Pr	-Prandtl number, [-]	c	-cold
Re	-Reynolds number, [UH / υ]	eff	-effective
s	-local coordinate around the fin[-]	h	-hot
T	-Temperature, [K]	k	-lattice model direction
t	-Time step,[s]	s	-sound
u	-velocity component,[m / s]	avg	-average
x	-Dimension,[m]	w	-wall
		Superscript	
		eq	-equilibrium distribution function

References

[1] Bejan, A. 2004. *Convection Heat Transfer*. Wiley, John & Sons.

[2] Nield, D. A., and A. Bejan. 2006. *Convection in Porous Media*. New York: Springer.

[3] Vafai, K. 2005. *Handbook of Porous Media*. Taylor & Francis.

[4] Hwang, G. J. and C. H. Chao. 1994. Heat Transfer Measurement and Analysis for Sintered Porous Channels. *Journal of Heat Transfer*. 116(2): 456–464.

[5] Jiang, P. X., M. Li, T. J. Lu, L. Yu, and Z.P. Ren. 2004. Experimental Research on Convection Heat Transfer in Sintered Porous Plate Channels. *International Journal of Heat and Mass Transfer*. 47(10-11): 2085–2096.

[6] Jiang, P.X., and X.C. Lu. 2006. Numerical Simulation of Fluid Flow and Convection Heat Transfer in Sintered Porous Plate Channels. *International Journal of Heat and Mass Transfer*. 49(9-10): 1685–1695.

[7] Shuja, S. Z., B. S. Yilbas, and M. Kassas. 2009. Flow Over Porous Blocks in a Square Cavity: Influence of Heat flux and Porosity on Heat Transfer Rates. *International Journal of Thermal Sciences*. 48(8): 1564–1573.

[8] Hadim, H., and M. North, 2005. Forced Convection in a Sintered Porous Channel with Inlet and Outlet Slots. *International Journal of Thermal Sciences*. 44(1): 33–42.

[9] Saeidi, S. M., and J. M. Khodadadi. 2007. Transient Flow and Heat Transfer Leading to Periodic State in a Cavity with Inlet and Outlet Ports Due to Incoming Flow Oscillation. *International Journal of Heat and Mass Transfer*. 50(3-4): 530–538.

[10] Saeidi, S. M., and J. M. Khodadadi. 2006. Forced Convection In A Square Cavity with Inlet and Outlet Ports. *International Journal of Heat and Mass Transfer*. 49(11): 1896–1906.

[11] Fattahi, E., M. Farhadi, and K. Sedighi. 2010. Lattice Boltzmann Simulation of Natural Convection Heat Transfer in Eccentric Annulus. *International Journal of Thermal Science*. 49(12): 2353–2362.

[12] Nemati, H., K. Sedighi, M. Farhadi, M. M. Pirouz, and E. Fattahi. 2010. Numerical Simulation of Fluid Flow of Two Rotating Side by Side Circular Cylinder by Lattice Boltzmann Method. *International Journal of Computational Fluid Dynamic*. 24(3-4): 83–94.

[13] Shan, X. and H. Chen. 1993. Lattice Boltzmann Model for Simulating Flows with Multiple Phases and Components. *Physical Review E*. 47(3): 1815–1819.

[14] Abouei Mehrizi, A., M. Farhadi, H. Hassanzade afroozi, K. Sedighi, and A.A. Rabienataj Darzi. 2012. Mixed Convection Heat Transfer in a Ventilated Cavity with Hot Obstacle: Effect of Nanofluid and Outlet Port Location. *International Communication in Heat and Mass Transfer*. In Press, doi:10.1016/j.icheatmasstransfer.2012.04.002.

[15] Huber, H., A. Parmigiani, B. Chopard, M. Manga and O. Bachmann, 2008. Lattice Boltzmann Model for Melting with Natural Convection. *International Journal of Heat and Fluid Flow* 29: 1469–1480.

[16] Delavar, M. A., M. Farhadi, and K. Sedighi. 2010. Numerical Simulation of Direct Methanol Fuel Cells Using Lattice Boltzmann Method. *International Journal of Hydrogen Energy*. 35(17): 9306–9317.

[17] Guo, Z., and T. S. Zhao, 2002. Lattice Boltzmann Model for Incompressible Flows Through Porous Media. *Physical Revew E*. 66(3): 036304.

[18] Seta, T., E. Takegoshi, K. Kitano, and K. Okui, 2006. Thermal Lattice Boltzmann Model for Incompressible Flows Through Porous Media. *Journal of Thermal Science and Technology*. 1(2): 90–100.

[19] Seta, T., E.Takegoshi and K. Okui, 2006. Lattice Boltzmann Simulation of Natural Convection in Porous Media. Mathematics and Computers in Simulation. 72(2-6): 195–200.

[20] Javaran, J., S. A. Gandjalikhan Nassab and S. Jafari. 2010. Thermal Analysis of a 2-D Heat Recovery System Using Porous Media Including Lattice Boltzmann Simulation of Fluid Flow. *International Journal of Thermal Science*. 49(6): 1031–1041.

[21] Nield, D. A. and A. V. Kuznetsov. 2005. Thermally Developing Forced Convection in a Channel Occupied by a Porous Medium Saturated by A Non-Newtonian Fluid. *International Journal of Heat and Mass Transfer*. 48(6): 1214–1218.

[22] Ergun, S. 1952. Flow through Packed Columns. *Chemical Engineering and Processing*. 48(2): 89.

[23] Peng, Y., C. Shu and Y. T Chew. 2004. A 3D Incompressible Thermal Lattice Boltzmann Model and Its Application to Simulate Natural Convection in a Cubic Cavity. *Journal of Computational Physics*. 193(1): 260–274.

[24] Mahmud, S. and R. A. Fraser, 2005. Flow, Thermal, and Entropy Generation Characteristics Inside a Porous Channel with Viscous Dissipation. *International Journal of Thermal Science*. 44(1): 21–32.

[25] Nithiarasu, P., K. N. Seetharamu and T. Sundararajan, 1997. Natural Convective Heat Transfer in a Fluid Saturated Variable Porosity Medium. *International Journal of Heat and Mass Transfer*. 40(16): 3955–3967.